NASA Technical Memorandum 102075

Photovoltaic Power System Operation in the Mars Environment

Joseph Appelbaum and Dennis J. Flood
Lewis Research Center
Cleveland, Ohio

Prepared for the
24th Intersociety Energy Conversion Engineering Conference
cosponsored by the IEEE, AIAA, ANS, ASME, SAE, ACS, and AIChE
Washington, D.C., August 6–11, 1989

NASA

PHOTOVOLTAIC POWER SYSTEM OPERATION IN THE MARS ENVIRONMENT

Joseph Appelbaum* and Dennis J. Flood
National Aeronautics and Space Administration
Lewis Research Center
Cleveland, Ohio 44135

ABSTRACT

Detailed information on the environmental conditions on Mars are very desirable for the design of photovoltaic systems for establishing outposts on the Martian surface. This paper addresses the variation of solar insolation (global, direct and diffuse) at the Viking lander's locations and can also be used, to a first approximation, for other latitudes. The radiation data is based on measured optical depth of the Martian atmosphere derived from images taken of the sun with a special diode on the Viking cameras; and computation based on multiple wavelength and multiple scattering of the solar radiation. The data are used to make estimates of photovoltaic system power, area and mass for a surface power system using regenerative fuel cells for storage and nighttime operation.

E-4740

INTRODUCTION

NASA, through its Project Pathfinder, has put in place a wide-ranging set of advanced technology programs to address future needs of manned space exploration. Included in the mission sets under study is the establishment of outposts on the surface of Mars. The Surface Power Program in Pathfinder is aimed at providing ultralightweight photovoltaic array technology for such an application (as well as for the lunar surface). Detailed information on the climatic conditions on Mars at the photovoltaic system location is very desirable. These include the variation of solar insolation; ambient temperature; albedo; and wind speeds and directions; with latitude, season, and time of the day. In addition, the effect of dust accumulation on the photovoltaic panels and radiation damage causing degradation of the output power needs to be assessed.

As on the planet Earth, the solar radiation on the surface of Mars is composed of two components: the direct beam, and diffuse component. The direct beam is affected by scattering and absorption along the path from the top of the Martian atmosphere to the Martian surface. Measurement of the optical depth [1,2] of the Martian atmosphere allows an estimate of the absorption and scattering out of the beam. These estimates were derived from images taken of the Sun and the Sun and Phobos with a special diode on the Viking lander cameras. Since the cameras are sitting on the Martian surface, the measured intensity is directly related by Beer's law to the optical depth of the intervening atmospheric haze:

$$G_b = G_o \exp\left[-\frac{\tau}{m(z)}\right] \qquad (1)$$

where G_o is the unattenuated irradiance at the top of the Martian atmosphere; G_b is the direct beam irradiance on Martian surface normal to the solar rays; τ is the optical depth; and $[m(z)]^{-1}$ is the airmass determined by the zenith angle z.

Earth-terrestial insolation data are accumulated over many years at different locations around the world and are given as long term average values. The optical depth data for Mars are derived for less than two Mars years. Consequently, the calculated solar insolation corresponds to short term data. Furthermore, the measured opacities (optical depth) and the calculated irradiances pertain to just two locations on the Mars planet; Viking lander 1 (VL1), located at 22.3° N latitude and 47.7° W longitude, and Viking lander 2 (VL2), located at 47.7° N latitude and 225.7° W longitude. However, the similarity in the properties of the dust suspended above the two landing sites suggests that they are also representative of ones at other locations, at least, at latitudes not too far from the lander's sites. Data from lander VL1 may be used for latitudes 40° N to 40° S and data from lander VL2 for higher latitudes. The Martian atmosphere consists mainly of suspended dust particles, the amounts of which vary daily, seasonally, and annually, depending on local and global storm intensities and their duration. The optical depth values given in the section entitled OPTICAL DEPTH are assumed to be constant throughout the day. Large values of optical depth correspond to global storms, i.e., days with low insolation ("dark days").

The albedo of the Martian surface varies in the range of about 0.1 to 0.4. The irradiances derived in the section entitled SOLAR RADIATION correspond to 0.1 albedo but can be also used for other values of albedo, to the first approximation.

In this paper we calculated the variation of solar irradiance which is the major environmental component for photovoltaic system design. We do not report here data on ambient temperature, wind speed and direction, albedo and the effect of dust

*This work was done while the author was a National Research Council -- NASA Research Associate; on sabbatical leave from Tel Aviv University.

New information about Mars climate may be forthcoming in the future based on new analysis, observations and future flight missions. The Mars climatic data for photovoltaic system design will thus be updated accordingly.

We have also completed a preliminary calculation of photovoltaic power system size and mass (including storage), based on the data now in hand, for use on the Martian surface during a so-called "sprint" mission (i.e., 30 day duration or less on the surface). The detailed assumptions appear in the last section of the paper on power system considerations, and the results appear in Table II.

OPTICAL DEPTH

The most direct and probably reliable estimates of opacity are those derived from Viking lander imaging of the Sun. Figures 1 and 2 show the seasonal variation of the normal-incidence of the optical depth at the Viking lander locations VL1 and VL2, respectively. The season is indicated by the value of L_s, areocentric longitude of the Sun, measured in the orbital plane of the planet from its vernal equinox (L_s = 0° and 180° corresponding to spring and fall equinox for the northern hemisphere, respectively; and L_s = 90 and 270° corresponding to northern and southern summer solstices, respectively). Figures 1 and 2 were derived from references by Pollack [1,2] and Zurek [3] and were discretized for each 5°. As mentioned before, the optical depth is assumed to remain constant throughout the day. Opacities are minimum during the northern spring (L_s = 0° to 90°) and summer (L_s = 90° to 180°), and maximum during southern spring (L_s = 180° to 270°) and summer (L_s = 270° to 360°), the seasons during which most local and major dust storms occur. When dust storms are not present, the optical depth are typically about 0.5. Two global dust storms occurred during the period of the observation as indicated by the high values of the optical depth (lower bound values).

GLOBAL AND LOCAL DUST STORMS

The intensity of Martian global and local dust storms is defined in terms of opacity of the dust it raises. Global dust storms are those which obscure planetary-scale sections of the Martian surface for many Martian days (sols), whereas local dust storms are less intense, and form and dissipate in a few days or less. From photovoltaic system design point of view, the intensity, frequency, and duration of these storms may be viewed as "partially cloudy" and "cloudy" days for which additional energy storage in the photovoltaic system must be taken into account. The characteristics of global and local dust storms are listed below.

Global Dust Storms

(1) One, or occasionally two global dust storms of planetary scale may occur each Martian year. The duration may vary from 35 to 70 days or more. Although global dust storms do not occur every year, their occurrence is fairly frequent.

(2) Global dust storms begin near perihelion, when solar insolation is maximum (southern spring and summer) in the southern mid-latitude.

(3) The first global dust storm observed by VL (1977) spread from a latitude of 40° S to a latitude 48° N in about 5 to 6 days.

(4) The opacity during the global dust storm is greater than 1.

Local Dust Storms

(1) Local dust storms occur at almost all latitudes and throughout the year. However, they have been observed to occur most frequently in the approximate latitude belt 10° to 20° N and 20° to 40° S, with more dust clouds seen in the south than in the north, the majority of which occurred during southern spring.

(2) Based on Viking orbiter observations, it is estimated that approximately 100 local storms occur in a given Martian year.

(3) Local dust storms last a few days.

(4) The opacity of local dust storms may be assumed about 1.

SOLAR RADIATION

The solar insolation on the surface of Mars is composed of the direct beam and the diffuse components. The net solar flux integrated over the solar spectrum, on the Martian surface was calculated by Pollack [5] based on multiple wavelength and multiple scattering of the solar radiation. Derived data of this calculation is shown in Table I by the "normalized net flux function" $f(z,\tau)$ where the parameters are the zenith angle z and the optical depth τ. This table pertains to albedo of 0.1 but can be used for higher albedo values to a first approximation. Using these data we calculated the global solar irradiance. We assumed that the diffuse irradiance is obtained by subtracting the beam from the global irradiance.

The solar irradiance components, on a horizontal Martian surface, are related by:

$$G_h = G_{bh} + G_{dh} \qquad (2)$$

where

G_h global irradiance on a horizontal surface
G_{bh} direct beam irradiance on a horizontal surface
G_{dh} diffuse irradiance on a horizontal surface

The diffuse irradiance of the Martian atmosphere may be a result of a different mechanism than that for the Earth atmosphere, nevertheless, to a first approximation, we will apply Eq. (2) as for Earth-terrestrial calculations. The beam irradiance G_{bh} on a horizontal surface is given by:

$$G_{bh} = G_o \cos z \exp\left(\frac{-\tau}{m(z)}\right) \qquad (3)$$

For zenith angles $z < 70°$ one can approximate the airmass by:

$$\frac{1}{m(z)} \cong \frac{1}{\cos z} \tag{4}$$

The beam irradiance at the top of the Martian atmosphere is given by:

$$G_o = \frac{S}{r^2} \tag{5}$$

where S is the solar constant at the mean Sun-Earth distance of 1 AU, i.e., $S = 1371\ W/m^2$; r is the instantaneous Sun-Mars distance (heliocentric distance) given by [6]:

$$r = \frac{a(1 - e^2)}{1 + e \cos \theta} \tag{6}$$

where a is the Mars semimajor axis, and e is the Mars eccentricity, i.e., $e = 0.093377$; and θ is the true anomaly given by:

$$\theta = L_s - 248° \tag{7}$$

where L_s is the areocentric longitude and 248° is the areocentric longitude of Mars perihelion. The Sun-Mars mean distance in AU units is 1.5236915, therefore, the mean beam irradiance at the top of Mars atmosphere is: $1371/1.5236915^2 = 590\ W/m^2$. The instantaneous beam irradiance is given by Eqs. (5) to (7):

$$G_o = 590 \frac{\left[1 + e \cos(L_s - 248°)\right]^2}{\left(1 - e^2\right)^2} \tag{8}$$

and is shown in Fig. 3.

The global irradiance G_h on a horizontal Martian surface is obtained by:

$$G_h = G_o \frac{f(z,\tau)}{0.9} \cos z \tag{9}$$

The cosine of the zenith angle is:

$$\cos z = \sin \phi \sin \delta + \cos \phi \cos \delta \cos \omega \tag{10}$$

where

ϕ latitude
δ declination angle
ω hour angle

The solar declination angle is given by:

$$\sin \delta = \sin \delta_o \sin L_s \tag{11}$$

where $\delta_o = 24.936°$ is the Mars obliquity of rotation axis. The variation of the solar declination angle is shown in Fig. 4.

The relation between the planet solar time T and the hour angle ω, is shown in Fig. 5 and is given by:

$$\omega = 15T - 180 \tag{12}$$

where ω is measured from the true noon westward.

The following figures of solar irradiances were calculated based on Table I data and the mean irradiance of $590\ W/m^2$. Figures 6 to 8 describe the variation of the global, beam and diffuse irradiances, respectively, on a horizontal Martian surface; and are given in pairs as function of the optical depth τ, and zenith angle z. The variation of the global irradiance G_h, Eq. (9), is shown in Figs. 6(a) and (b). The beam irradiance G_{bh} is obtained using Eq. (3) and is shown in Figs. 7(a) and (b). The beam irradiance shows a sharp decrease with increasing optical depth, and a relative moderate decrease with increasing zenith angle. The diffuse irradiance G_{dh} is obtained from Eqs. (2), (3) and (9) and is shown in Figs. 8(a) and (b). The diffuse irradiance shows a sliding maximum with the variation of the zenith angle.

For a given day L_s and latitude ϕ, one can calculate the variation of the zenith angle z as function of the solar time T using Eqs. (10) to (12). Referring to Figs. 1 and 2 for the given L_s, the optical depth τ is determined, and using Figs. 6 to 8 one can calculate the variation of the solar irradiance for the given day. The results of such a procedure is shown, for example, in Fig. 9 where the variation of the global, beam and diffuse irradiance on a horizontal surface is depicted as function of the solar time for $L_s = 153°$ and at Viking lander VL1.

POWER SYSTEM CONSIDERATIONS FOR MARTIAN SURFACE OPERATION

The data presented in this paper represent a start on a longer term effort to provide a more complete analysis of temperature and insolation levels on Mars. The purpose for doing so is two-fold: (1) to establish the feasibility of using photovoltaic power systems on the surface of Mars, and (2) to allow for much more accurate calculations of critical power system characteristics, such as area and mass, than has been possible in the past. Of major concern are the dust storms, which have been observed to occur on local as well as global scales, and their effect on solar array output. In general, the assumption has been that global storms would reduce solar array output essentially to zero, because the opacity of the atmosphere may rise to values ranging from 3 to 9, depending on the severity of the storm. Furthermore, such high values of opacity may persist for long periods of time (often several weeks), so that predicted requirements for energy storage quickly become much too large to be practical. As shown in the preceding discussion, however, the opacity primarily affects the direct beam component of the solar radiation. Hence there is still an appreciably large diffuse component, even at an atmospheric opacity of 4 (Fig. 8), with the result that solar array operation is still possible. According to the data shown in the figure, array output at midday could be expected to be over 40 percent of its "clear weather" midday output during the height of that particular storm.

The second, and primary use for data such as are presented here, is to allow for more accurate estimates of photovoltaic power system sizes and masses in system analysis and trade-off studies. Ultimately, of course, such data will be required for final engineering design should a manned mission to Mars actually be attempted at some future date. Prior to any such actual engineering phase, however, it is important to analyze and compare all the relevant technology options, and to select those which look most favorable for further study and development. As an example, a comparison will be made of array areas and masses for two radically different solar cell options. It is assumed that energy storage will be provided by regenerative fuel cells (RFC) using hydrogen and oxygen as reactants. The storage system efficiency in this calculation takes into account the storage "round-trip" efficiency as well as the power management and distribution efficiencies. For storage times on the order of 10 hr or more, RFC energy storage densities have been shown to approach 1000 W-hr/kg [7]. The two solar cell options are thin film amorphous silicon at 12 percent AMO efficiency, and thin, single crystal GaAs cells at 26 percent AMO. Both cell types are assumed to be integrated into a suitable lightweight, flexible blanket assembly. Based on projections from the NASA Advanced Photovoltaic Solar Array Study [8], the GaAs blanket specific mass is calculated to be 0.5 kg/m^2, and the αSi blanket specific mass is 0.04 kg/m^2. The array structure in both cases is assumed to have a mass of 0.56 kg/m^2 meter of array area, to which must be added the blanket mass for each case. No temperature effects are included in this calculation, and it is assumed that the efficiencies quoted are at the expected operating temperature of the array. Also, not included is the mass of the power conditioning and distribution equipment for the loads on the power system.

The insolation level and opacity data are that observed by VL1 on day L_S = 153°. The actual irradiance level of 590 W/m^2 during this portion of Mar's orbit is approximately equal to the orbital mean value, and remains within 10 percent of that value for several weeks on either side of that day. It is also a period of relatively stable atmospheric conditions, with opacities around 0.5 for several days at a time. Figure 9 shows the variation with zenith angle of the irradiance on a fixed horizontal surface for that same day. Table II compares the area and mass of the two solar array types when both are fixed and horizontal, as might be the case if operational simplicity is desired for their deployment.

Array power per unit area and unit mass have been calculated with the condition that the array must provide its full rated output of 25 kWe for at least 5.5 hr past Martian noon, at which time the solar irradiance is 70 W/m^2 on the day selected. The ratio of the integrated total energy to the peak solar insolation is 0.59, which yields a daily average irradiance of 0.348 kW/m^2. It is interesting to note that although the mass of the αSi blanket was calculated to be less than 10 percent of the GaAs blanket, the αSi system mass is nearly 20 percent greater than the GaAs system mass. The reason is, of course, that the lower efficiency projected for αSi results in a much larger total area, and hence total mass, for that array, under the assumption that the same structural mass is required in each case. Clearly, a more detailed design is required to resolve the issue.

CONCLUSIONS

The major environmental parameter needed for photovoltaic system design is the variation of the solar insolation. The data and procedure from which the solar insolation can be determined is given in this paper, and is based on the normalized net solar flux function $f(z,\tau)$. The opacities were measured at the two Viking lander locations but can also be used, to the first approximation, for other locations. Figures 6 to 9 show the global, beam and diffuse irradiances on the horizontal surface. Any desired insolation quantities on any inclined surface can be further derived based on the $f(z,\tau)$ function and the appropriate solar calculations.

An example is presented for a surface power system using regenerative fuel cells for storage, and two different array types--one with GaAs cells, and one with αSi thin film cells. The results demonstrate the ease with which the solar insolation data provided here can be used to determine important power system parameters for system comparison studies, and for final engineering design.

ACKNOWLEDGMENT

We are very grateful to James B. Pollack from the Space Science Division, NASA Ames Research Center for supplying us with the data from which the $f(z,\tau)$ table was derived.

REFERENCES

[1] J.B. Pollack, et al., "Properties of Aerosols in the Martian Atmosphere, as Inferred from Viking Lander Imaging Data," Journal of Geographical Research, Vol. 82, No. 28, pp. 4479-4496, 1977.

[2] J.B. Pollack, et al., "Properties and Effects of Dust Particles Suspended in the Martian Atmosphere," Journal of Geographical Research, Vol. 84, No. B6, pp. 2929-2945, 1979.

[3] R.W. Zurek, Martian Great Dust Storms: An Update," ICARUS, Vol. 50, pp. 288-310, 1982.

[4] J.E. Tillman, Director and N.C. Johnson Viking Computer Facility, Department of Atmospheric Sciences, University of Washington, Seattle, Washington, private communication.

[5] J.B. Pollack, R.M. Harberle, J. Schaeffer and H. Lee, "Simulation of the General Circulation of the Martian Atmosphere I: Polar Processes," J. Geophys. Res. In press.

[6] E.V.P. Smith and K.C. Jacobs, Introductory Astronomy and Astrophysics, W.B. Saunders Co., 1973.

[7] L. Thaller, Private Communication, NASA Lewis Research Center.

[8] R.M. Kurland et al, "Advanced Photovoltaic Solar Array Design," 22nd IECEC Conference Proceedings, vol. I, Aug. 1987, pp. 103-114.

TABLE I. - NORMALIZED NET FLUX FUNCTION $f(z,\tau)$ AT THE MARTIAN SURFACE

Optical depth, τ	Zenith angle, z, deg.									
	0	10	20	30	40	50	60	70	80	85
0.1	0.8847	0.8829	0.8782	0.8772	0.8761	0.8662	0.8542	0.8385	0.7730	0.5600
0.5	.8085	.8039	.7922	.7891	.7786	.7523	.6956	.6422	.4832	.3800
1.0	.7261	.7187	.7061	.6958	.6671	.6289	.5644	.4817	.2818	.2600
2.0	.5797	.5747	.5600	.5337	.4899	.4390	.3722	.3033	.2196	.1500
3.0	.4637	.4600	.4415	.4192	.3783	.3275	.2654	.2052	.1669	.0950
4.0	.3737	.3687	.3523	.3347	.2987	.2492	.1983	.1427	.1142	.0650
5.0	.2959	.2912	.2776	.2642	.2350	.1946	.1556	.1249	.0878	.0480
6.0	.2288	.2277	.2191	.2061	.1852	.1566	.1342	.1026	.0703	.0350

TABLE II. - MARS MISSION POWER SYSTEM COMPARISON

Total power delivered to load (kWe): 25
Solar irrandance (kW/m^2): 0.348 (daily ave.).

(a) Performance parameters

Technology	Array			RFC energy storage mass, kg	System total			Array sized needed, KW
	m^2/kWe	kg/kWe	Mass-kg		Area-m^2	Mass-kg	kg/kWe	
Mars/Ground/GaAs/RFC	65.0	69.1	1728	516	1624	2244	89.9	135
Mars/Ground/αSi/RFC	140.7	84.3	2107	527	3518	2634	105.4	135

(b) Input parameters

Technology	Cell efficiency	Packing factor	Eclipse-to-sun ratio	Eclipse time, hr	Storage efficiency	Storage mass, W-hr/kg	Array mass, kg/m^2	Distribution efficiency	Condition efficiency
Mars/Ground/GaAs/RFC	0.26	0.91	1.24	13.6	0.65	1000	1.06	0.97	0.95
Mars/Ground/αSi/RFC	0.12	0.91	1.24	13.6	0.65	1000	0.6	0.97	0.95

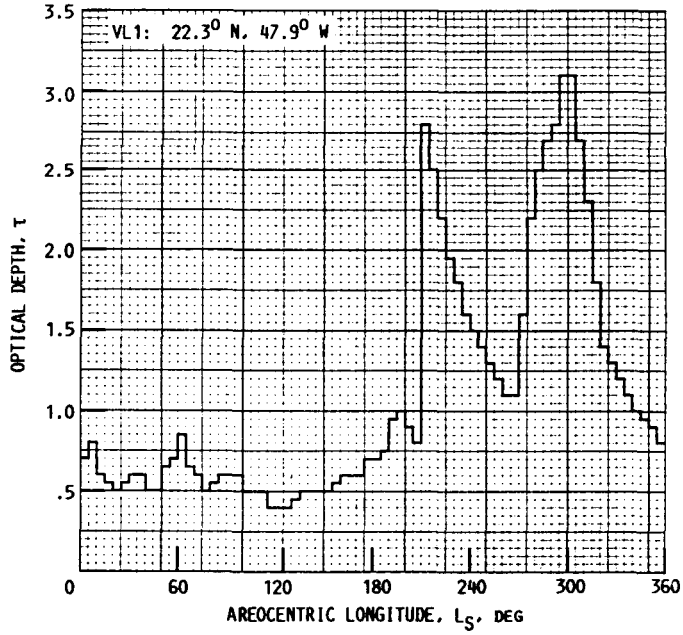

FIGURE 1. - OPTICAL DEPTH AS MEASURED FOR VIKING LANDER VL1 AS FUNCTION OF AREOCENTRIC LONGITUDE.

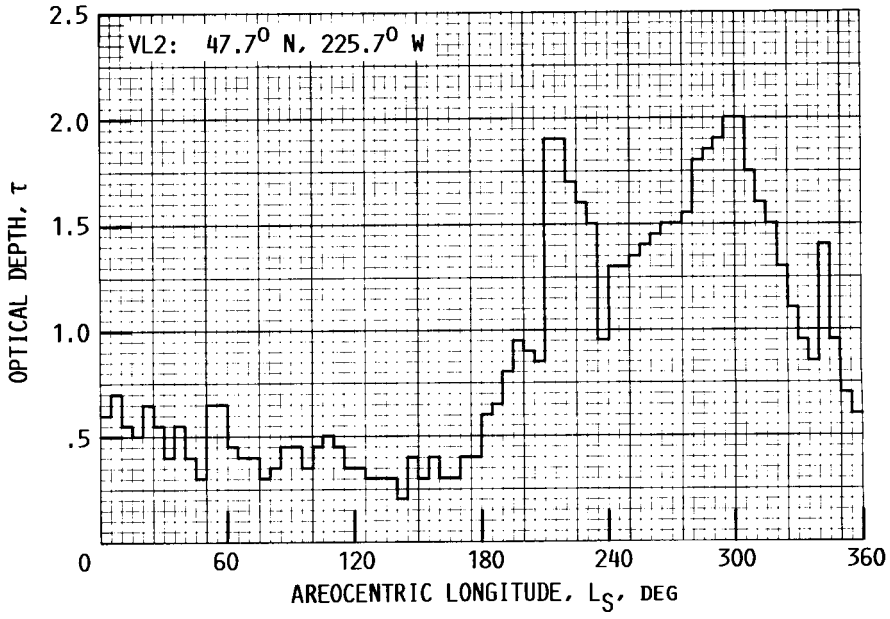

FIGURE 2. - OPTICAL DEPTH AS MEASURED FOR VIKING LANDER VL2 AS FUNCTION OF AREOCENTRIC LONGITUDE.

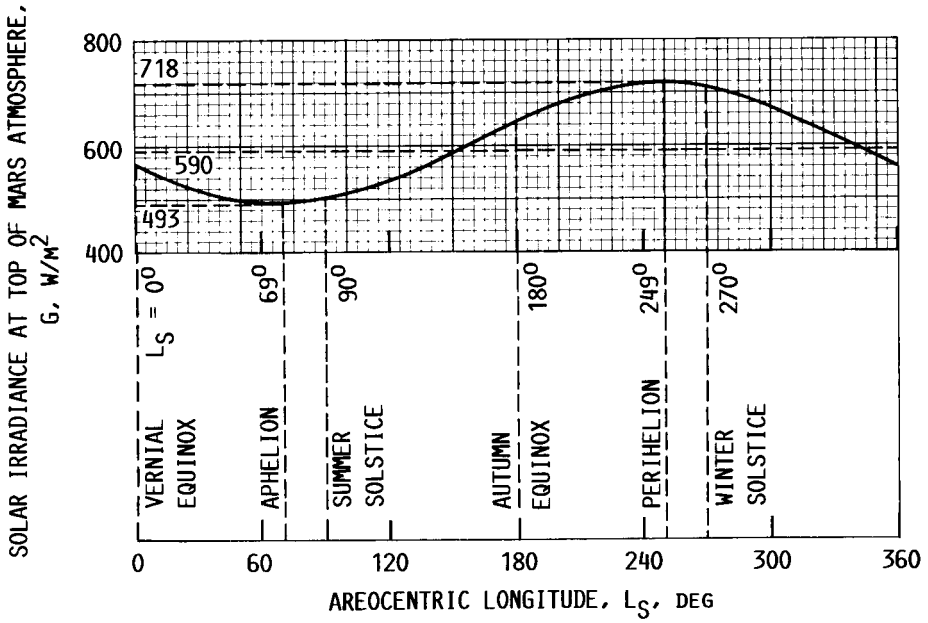

FIGURE 3. - SOLAR IRRADIANCE AT TOP OF MARS ATMOSPHERE AS FUNCTION OF AREOCENTRIC LONGITUDE.

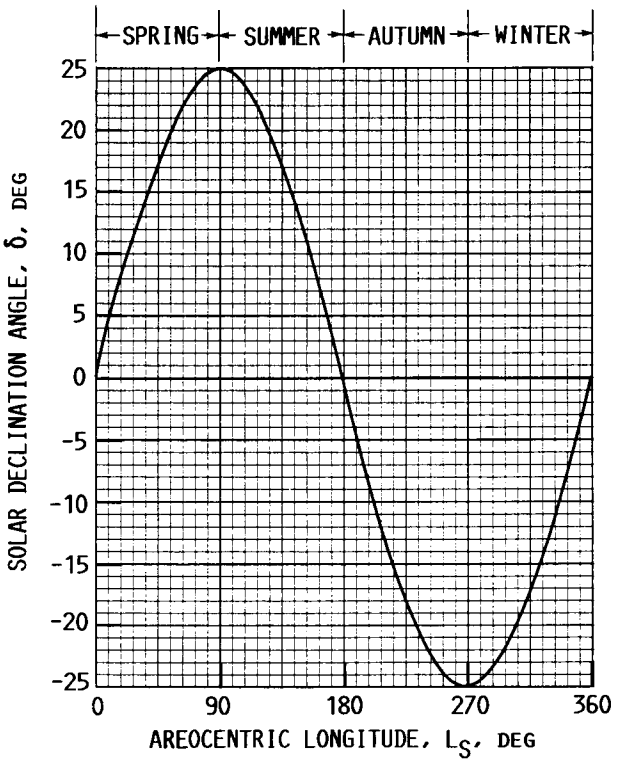

FIGURE 4. - VARIATION OF SOLAR DECLINATION ANGLE δ, WITH AREOCENTRIC LONGITUDE, L_S.

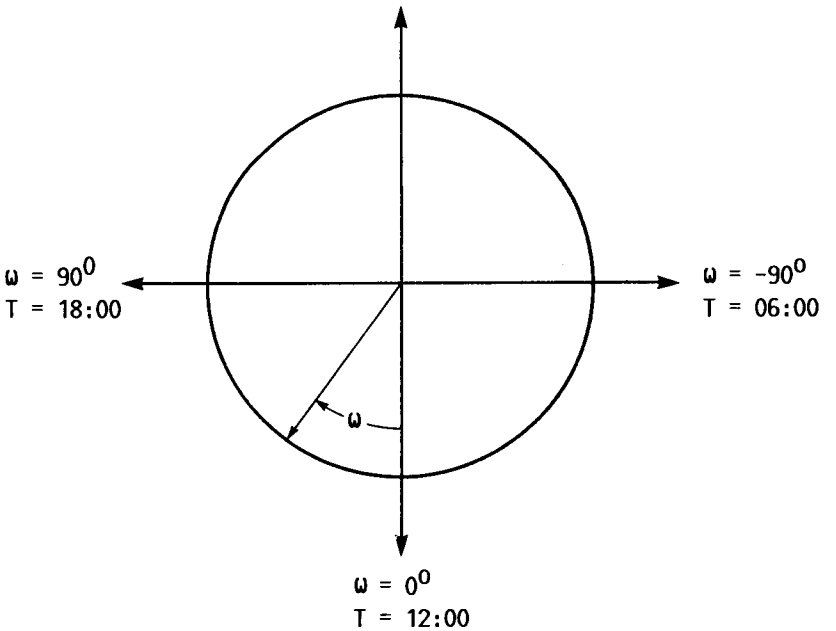

FIGURE 5. - SOLAR TIME AND HOUR ANGLE RELATION.

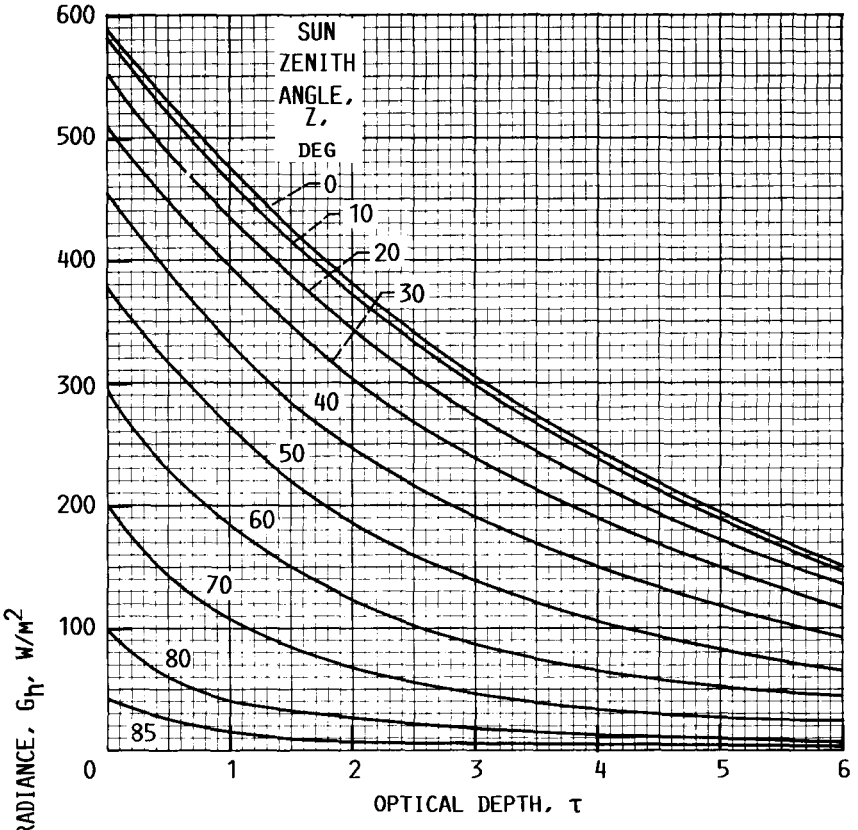

(A) EFFECT OF OPTICAL DEPTH WITH SUN ZENTH ANGLE AS A PARAMETER.

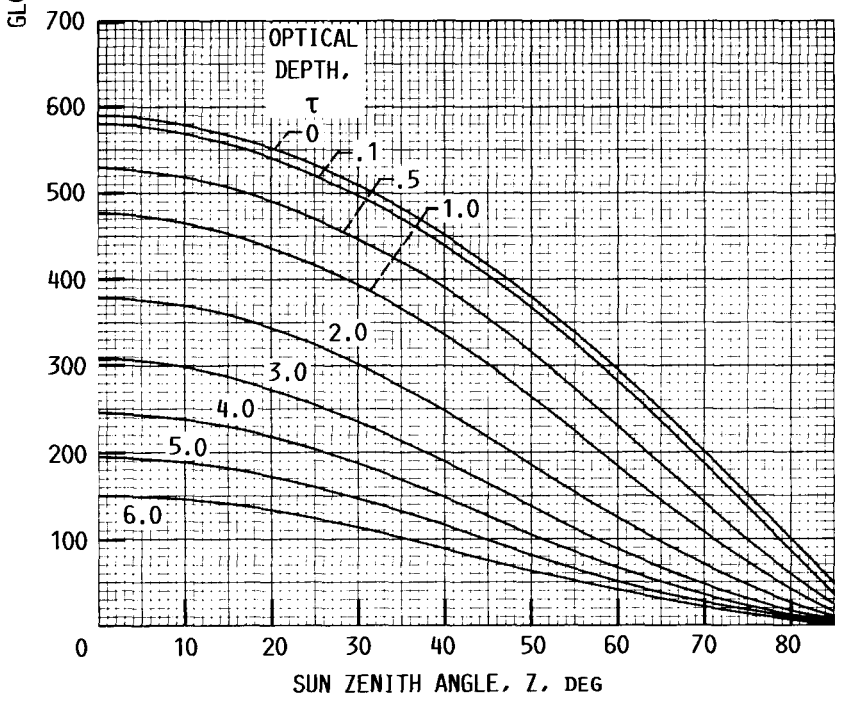

(B) EFFECT OF SUN ZENITH ANGLE WITH OPTICAL DEPTH AS A PARAMETER.

FIGURE 6. - VARIATION OF GLOBAL IRRADIANCE WITH OPTICAL DEPTH AND SUN ZENITH ANGLE ON A HORIZONTAL SURFACE.

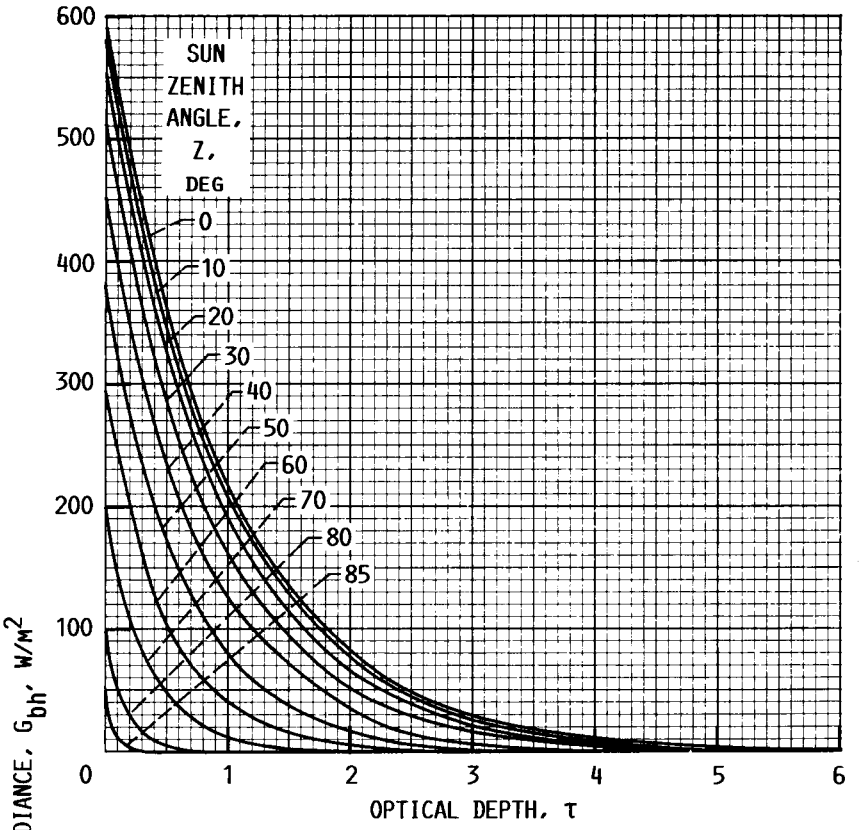

(A) EFFECT OF OPTICAL DEPTH WITH SUN ZENITH ANGLE AS A PARAMETER.

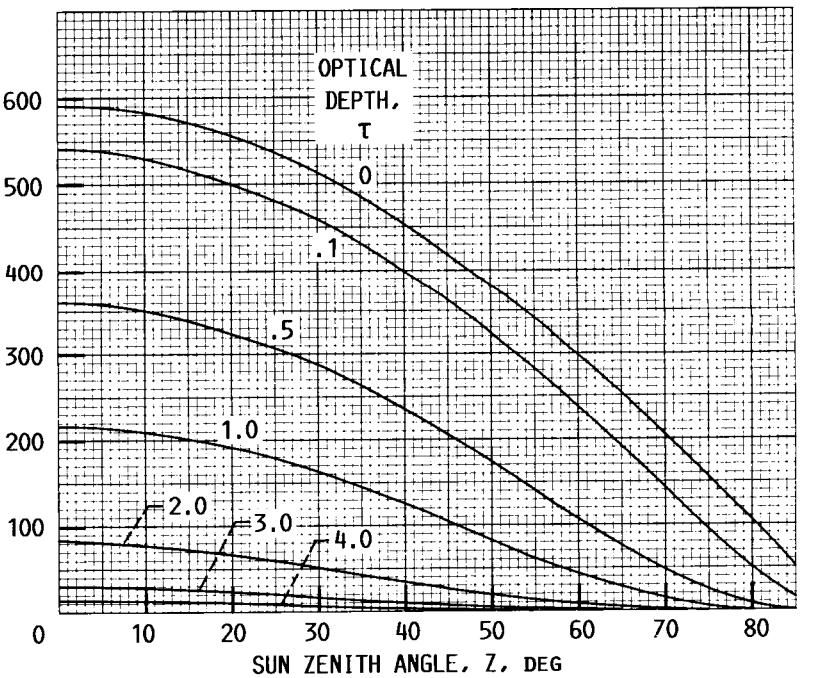

(B) EFFECT OF SUN ZENITH ANGLE WITH OPTICAL DEPTH AS A PARAMETER.

FIGURE 7. - VARIATION OF BEAM IRRADIANCE WITH OPTICAL DEPTH AND SUN ZENITH ANGLE ON A HORIZONTAL SURFACE.

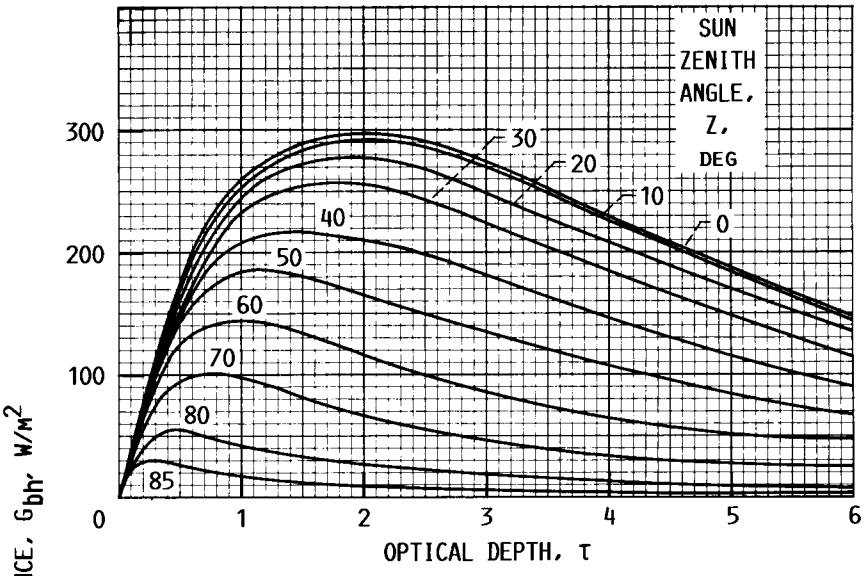

(A) EFFECT OF OPTICAL DEPTH WITH SUN ZENITH ANGLE AS A PARAMETER.

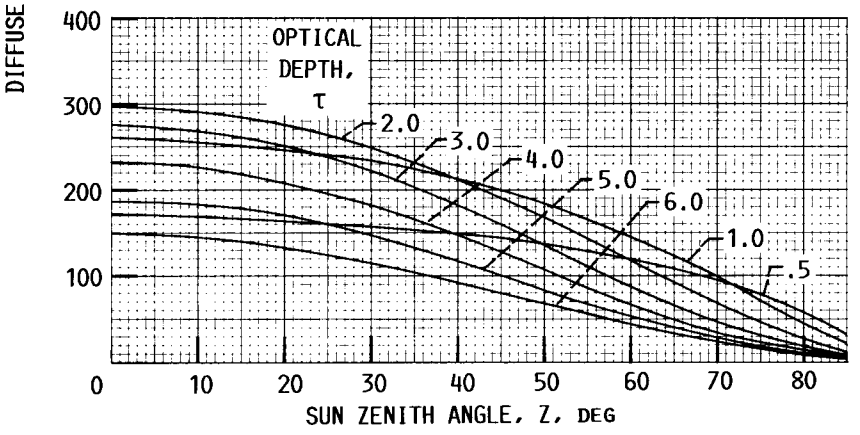

(B) EFFECT OF SUN ZENITH ANGLE WITH OPTICAL DEPTH AS A PARAMETER.

FIGURE 8. - VARIATION OF DIFFUSE IRRADIANCE WITH OPTICAL DEPTH AND SUN ZENITH ANGLE ON A HORIZONTAL SURFACE.

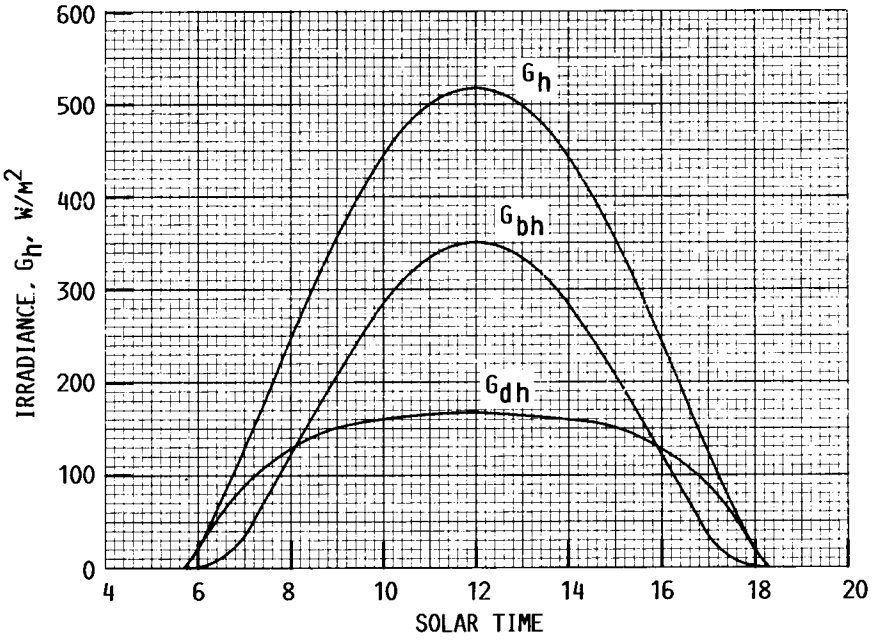

FIGURE 9. - DIURNAL VARIATION OF SOLAR IRRADIANCE ON A HORIZONTAL SURFACE AT VIKING LANDER VL1. AREOCENTRIC LONGITUDAL, 153; OPTICAL DEPTH, 0.5.

NASA
National Aeronautics and Space Administration

Report Documentation Page

1. Report No.	2. Government Accession No.	3. Recipient's Catalog No.
NASA TM-102075		

4. Title and Subtitle	5. Report Date
Photovoltaic Power System Operation in the Mars Environment	
	6. Performing Organization Code

7. Author(s)	8. Performing Organization Report No.
Joseph Appelbaum and Dennis J. Flood	E-4740
	10. Work Unit No. 506-41-11

9. Performing Organization Name and Address	11. Contract or Grant No.
National Aeronautics and Space Administration Lewis Research Center Cleveland, Ohio 44135-3191	
	13. Type of Report and Period Covered Technical Memorandum

12. Sponsoring Agency Name and Address	14. Sponsoring Agency Code
National Aeronautics and Space Administration Washington, D.C. 20546-0001	

15. Supplementary Notes

Prepared for the 24th Intersociety Energy Conversion Engineering Conference cosponsored by the IEEE, AIAA, ANS, ASME, SAE, ACS, and AIChE, Washington, D.C., August 6-11, 1989. Joseph Appelbaum, National Research Council-NASA Research Associate; on sabbatical leave from Tel Aviv University. Dennis J. Flood, NASA Lewis Research Center.

16. Abstract

Detailed information on the environmental conditions on Mars are very desirable for the design of photovoltaic systems for establishing outposts on the Martian surface. This paper addresses the variation of solar insolation (global, direct and diffuse) at the Viking lander's locations and can also be used, to a first approximation, for other latitudes. The radiation data is based on measured optical depth of the Martian atmosphere derived from images taken of the sun with a special diode on the Viking cameras; and computation based on multiple wavelength and multiple scattering of the solar radiation. The data are used to make estimates of photovoltaic system power, area and mass for a surface power system using regenerative fuel cells for storage and nighttime operation

17. Key Words (Suggested by Author(s))	18. Distribution Statement
Mars environment; Direct beam and diffuse insolation; Optical depth of Mars atmosphere; Solar cells; Photovoltaic power systems	Unclassified-Unlimited Subject Category 33

19. Security Classif. (of this report)	20. Security Classif. (of this page)	21. No of pages	22. Price*
Unclassified	Unclassified	12	A03

*For sale by the National Technical Information Service, Springfield, Virginia 22161